

## FAULT IDENTIFICATION IN FUEL CELLS BASED ON BAYESIAN NETWORK DIAGNOSIS

### Luis A.M. Riascos

Escola Politecnica da USP  
Av. Prof. Mello Moraes, 2231, São Paulo – SP, Brazil  
lriascos@usp.br

### Marcelo G. Simões

Colorado School of Mines  
1500 Illinois St, Golden – CO, USA  
mgs@mines.edu

### Paulo E. Miyagi

Escola Politecnica da USP  
Av. Prof. Mello Moraes, 2231, São Paulo – SP, Brazil  
pemiyagi@usp.br

**Abstract.** *This paper considers the effects of different types of faults on a model of a proton exchange membrane fuel cell (PEMFC). Using databases (which record the effects of the faults) and probabilistic methods (such as the Bayesian-Score and Markov Chain Monte Carlo), a graphical-probabilistic model for fault diagnosis is constructed. The graphical structure defines the cause-effect relationship among the variables, and the probabilistic method captures the numerical dependence among these variables. Finally, the Bayesian network (i.e. the graphical-probabilistic model) is used to execute the diagnosis of fault causes in the PEMFC based on observed effects. These effects can be monitored through sensors in the machine.*

**Keywords:** *Bayesian networks, fault diagnosis, fuel cells.*

### 1. Introduction

Major efforts to reduce greenhouse gas emission have increased the demand for pollution-free sources of energy. Fuel cells are electrochemical devices that generate electricity, similar to batteries, but which can be continuously fueled. Most recent developments in proton exchange membrane fuel cell (PEMFC) technology have made the best alternative for stationary and mobile applications in the range of up to 200 KW. They are characterized by high efficiency, high power density, no aggression to the environment, contains no moving parts, and superior reliability and durability.

Fuel cells (FCs) convert the energy contained in hydrogen directly to electricity with only water as the product of the reaction. Under certain pressure, hydrogen ( $H_2$ ) is supplied into a porous conductive electrode (the anode). The  $H_2$  spreads through the electrode until it reaches the catalytic layer of the anode, where it reacts to form protons and electrons. The  $H^+$  ions (or protons) flow through the electrolyte (solid membrane), the electrons pass through an external electrical circuit, producing electrical energy and heat. On the other side of the cell, the oxygen ( $O_2$ ) is spread through the cathode and reaches its catalytic layer. On this layer, the  $O_2$ ,  $H^+$  protons, and electrons produce liquid water and residual heat as sub-products (Laminie, 2000).

Several papers have been published considering FC operation in normal conditions; but only few of them addressed FC operation under fault analysis. Faults are events that cannot be ignored in any real machines, and their consideration is essential for improving the operability, flexibility, and autonomy of commercial equipment.

In this paper, Bayesian network algorithms are applied to construct a graphical-probabilistic model for fault diagnosis in PEMFCs from databases of fault records.

This paper is organized as follows. In section 2, the basic concepts for the mathematical model of a PEMFC are introduced. In section 3, four types of faults in PEMFC are considered: faults in the air reaction fan, faults in the cooling system, growth of the fuel crossover and internal loss current, and faults in the hydrogen feed line. Section 4 introduces a short background of Bayesian networks and learning algorithms to be applied on fault diagnosis of PEMFC.

### 2. The Fuel Cell Model

A mathematical model of a fuel cell (FC) was used to study the possible fault effects. This model consists of an electro-chemical and a thermo-dynamical sub-system.

#### 2.1 The Electrochemical Model

The output voltage of a single cell ( $V_{FC}$ ) can be defined as the result of the expression (Larminie, et al. 2000):

$$V_{FC} = E_{Nernst} - V_{act} - V_{ohmic} - V_{con} \quad (1)$$

$E_{Nernst}$  is the thermodynamic potential of the cell and it represents its reversible voltage.  $E_{Nernst}$  is a function of the hydrogen ( $P_{H_2}$ ), oxygen pressures ( $P_{O_2}$ ), and is the operating temperature.

$V_{act}$  is the voltage drop due to the activation of the anode and the cathode, and is a function of the coefficients  $\xi_i$  ( $i = 1..4$ ), which are specific for every type of FC, the electrical current ( $i_{FC}$ ), and the oxygen concentration ( $c_{O_2}$ ).

$V_{ohmic}$  is the ohmic voltage drop associated with the conduction of protons through the solid electrolyte, and of electrons through the internal electronic resistance, and is a function of the contact resistance to electron flow ( $R_C$ ) the resistance to proton transfer through the membrane ( $R_M$ ).  $R_M$  is a function of the specific resistivity of membrane ( $\rho_M$ ), the thickness of membrane ( $\ell$ ), the active area of the membrane ( $A$ ) and the coefficient  $\psi$  which depend on the type of membrane.

$V_{con}$  represents the voltage drop resulting from the mass transportation effects, which affects the concentration of the reacting gases, and is a function of the constant  $B$  which depend on the type of FC, the maximum electrical current density ( $J_{max}$ ), and the electrical current density produced by the cell ( $J$ ). In general,  $J=J_{out}+J_n$  where  $J_{out}$  is the real electrical output current density, and  $J_n$  is the fuel crossover and internal loss current.

Considering a stack composed by several FCs, the output voltage is:  $V_S=nr \cdot V_{FC}$ , where  $nr$  is the number of cells composing the stack. Those equations are described in detail in (Correa, et al. 2003).

In this paper, a mathematical model for a 500-Watts stack (manufactured by BCS Technologies) is used. The parameters for this particular model are presented in Table 1. In (Correa, et al. 2004) the polarization curve obtained with this model is compared to the polarization curve of the manufacturing data sheet to validate the model.

Table 1. Parameters of a PEMFC BCS, 500 (W)

parameter	Value	parameter	Value
$nr$	32	$\xi_1$	-0,948
$A$	64 (cm <sup>2</sup> )	$\xi_2$	0,00286+0,0002.ln A+(4,3.10 <sup>-5</sup> ).ln $c_{H_2}$
$\ell$	178 (μm)	$\xi_3$	7,6x10 <sup>-5</sup>
$P_{O_2}$	0.2095 (atm)	$\xi_4$	-1,93x10 <sup>-4</sup>
$P_{H_2}$	1 (atm)	$\psi$	23,0
$R_C$	0,003 (Ω)	$J_n$	3 (mA/cm <sup>2</sup> )
$B$	0,016 (V)	$J_{max}$	0.469 (A /cm <sup>2</sup> )

In general, these parameters are based on manufacturing data and laboratory experiments, and their accuracy can affect the simulation results. In (Correa, et al. 2005), a multi-parametric sensitivity analysis is performed to define the importance of the accuracy of each parameter. Basically, the parameters are classified in three groups: insensitive ( $A$ ,  $R_C$ ,  $\ell$ ), sensitive ( $J_n$ ,  $B$ ,  $\psi$ ,  $\xi_4$ ), and highly sensitive parameters ( $J_{max}$ ,  $\xi_3$ ,  $\xi_1$ ). The accuracy was analyzed in normal conditions, considering variations around  $\pm 10\%$  of their normal values. However, in faulty conditions, those variations can be stronger, as presented in sections 3.1 through 3.4.

## 2.2 The Thermo-Dynamical Model

The calculation of the relative humidity and the operating temperature of the FC compose essentially the thermo-dynamical model (Correa, et al. 2004).

### 2.2.1 Temperature

The variation of temperature is a function of the whole stack mass (Kg), the average specific heat coefficient of the stack ( $J/^\circ K \cdot kg$ ), and  $\Delta \dot{Q}$  (J/s) is the rate of heat variation (i.e. the difference between the rate of heat generated by the cell operation ( $\dot{Q}_{ger}$ ) and the rate of heat removed). Heat can be removed by the reaction air flowing in the stack ( $\dot{Q}_{rem_1}$ ) and by the cooling system ( $\dot{Q}_{rem_2}$ ). The possible contribution of water evaporation is not considered, and the heat exchanged with the surroundings is considered smaller than  $\dot{Q}_{rem_2}$ .

In this FC system, the refrigeration system is turned on when the operating temperature is higher than 50°C.

### 2.2.2 Relative Humidity

A correct level of humidity should be maintained in the FC. This level is measured through the relative humidity ( $UR$ ). If the  $UR$  is much less than 100%, then the membrane dries out and the conductivity decreases. On the other hand, a relative humidity greater than 100% produces accumulation of liquid water on the electrodes, which can become flooded and block the pores. This makes difficult the gas diffusion. The result of these two conditions is a fairly narrow range of normal operating conditions.

In abnormal conditions (such as flooding or drying), parameters (such as  $R_C$  and  $R_M$ ) that are normally constant (table 1) start to vary. Figure 1 (adapted from (Larminie, et al. 2000)) illustrates the variation of temperature and relative humidity for different stoichiometry air relationships ( $\lambda=2$ ,  $\lambda=4$ ). The stoichiometry ( $\lambda$ ) is the relationship between inlet air divided by the air necessary for the chemical reaction.

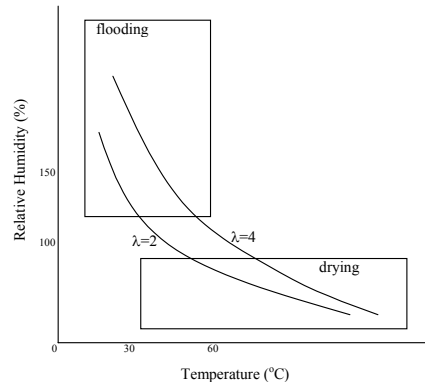


Figure 1. Temperature and relative humidity for  $\lambda=2$  e  $\lambda=4$ .

### 2.3 Normal Operation of a Fuel Cell

Figure 2 illustrates the evolution of a few PEMFC variables in normal operating conditions as a function of time. The variables are: Voltage, temperature (Temp), and volume of air Flow. In this test, the FC supports a constant-load demand; thus, the voltage and electrical current should vary by themselves to maintain this demand, (i.e. the output power would be constant).

The simulation begins with the FC system in stand-by (i.e. without load, and at environmental temperature, aprox. 25°C). After a load requirement, the electrical equilibrium is reached in less than 3 seconds (e.g. the equilibrium of voltage and current). On the other hand, the temperature begins to increase until, at  $t=10$  minutes, it reaches 50°C. Then, the refrigeration system is turned on. The temperature increases slowly until the thermo-dynamical steady state is reached after  $t=40$  minutes. Note that variations in voltage are performed, especially in the first 10 minutes, but they are produced by the evolution of the thermo-dynamical state.

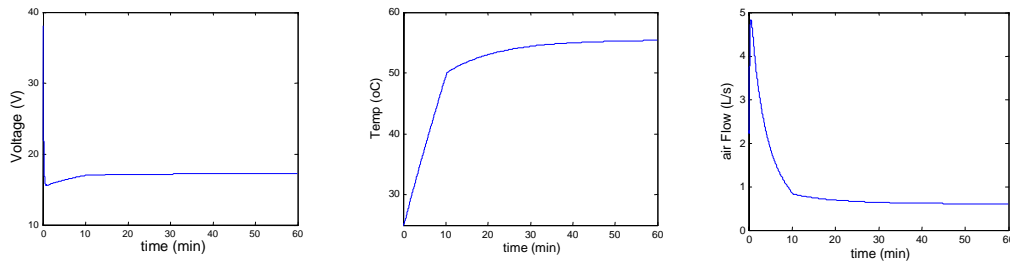


Figure 2. Evolution of variables of a PEMFC in normal conditions derived from a mathematical model in MATLAB®

### 3. Faults in Fuel Cells

In general, two types of fault detection can be considered:

- Faults that can be detected by monitoring a specific variable. For example, the leak of fuel can be detected installing a specific gas sensor. In this case a diagnosis is not necessary.
- Faults that cannot be detected directly by monitoring or faults that need some type of diagnosis.

In practice, fault detection on commercial fuel cell equipment is limited to detection of faults of the first type. This work focuses on fault detection of the second type.

Four types of faults in PEMFCs are considered: 1) fault in the air reaction fan, 2) fault in the cooling system, 3) growth of the fuel crossover and internal loss current, and 4) fault in the hydrogen feed line. The effects of these faults are included in the mathematical model to analyze the behavior of the FC system in fault operating conditions.

#### 3.1 Faults in the Air Reaction Fan

A reduction of the reaction air by a fault in the air fan can produce two major effects: (i) accumulation of liquid water than cannot be evaporated, and (ii) reduction of O<sub>2</sub> volume below necessary for a complete reaction with the H<sub>2</sub>. A common method for removing excess water inside the FC is using the air flowing through it. The correct variation of the stoichiometry ( $\lambda$ ) maintains the UR proximal to 100%. However, when a fault in the air reaction fan takes place, this becomes impossible. This fault reduces the air reaction flow, which reduces the water evaporation volume and permits the accumulation of water. A great accumulation of water produces flooding of electrodes, which changes the resistance of electrodes to electron flow ( $R_C$ ). The  $R_C$  changes according to equation (2):

$$R_{C(k)} = R_{C(0)} \cdot \sqrt{\frac{W_{acum(k)}}{const_1}} \quad (2)$$

where:  $R_{C(0)}$  is the value of the variable at the initial state (normal condition),  $w_{acum(k)}$  is the volume of water accumulated at instant  $k$ , and  $const_1$  is a constant defining when the electrodes are taken to be flooded.

This variation of  $R_C$  produces an increase in the  $V_{ohmic}$  and consequently reduces the output voltage of the FC ( $V_{FC}$ ).

The second effect of a fault in the air reaction fan occurs when  $\lambda$  is below the practical and recommended value. In this case, the  $O_2$  concentration is reduced and the exit air can be completely depleted of  $O_2$ . This reduction of  $O_2$  concentration produces a negative effect on the  $E_{Nernst}$  and an increment on the  $V_{act}$ .

In this case, the  $O_2$  concentration changes according to equation (3):

$$c_{O_2(k)} = \frac{c_{O_2(0)}}{\sqrt{\frac{const_2}{\lambda_{(k)}}}} \quad (3)$$

where:  $c_{O_2(k)}$  is the  $O_2$  concentration at instant  $k$ ,  $c_{O_2(0)}$  is the normal  $O_2$  concentration in the air, and  $const_2$  is a constant defining when  $\lambda$  is lower than necessary for the reaction.

Figure 3 illustrates the evolution of a few variables when a fault in the reaction air fan is considered. The variables are Voltage, Temperature, air Flow, and accumulated water. In this case, the starting point of the simulation ( $t=0$ ) is an FC on thermal steady state. The fault in the air reaction fan takes place at  $t=30$  minutes. The initial effect is the variation of the air flow volume. This affects the performance of the FC and varies the  $I_{FC}$ . This fault produces accumulation of liquid water and, at  $t = 45$  minutes, the accumulation of water is enough to produce variation on the resistance of electrodes. Then it produces a continuous variation on variables such as Voltage and, consequently  $I_{FC}$ .

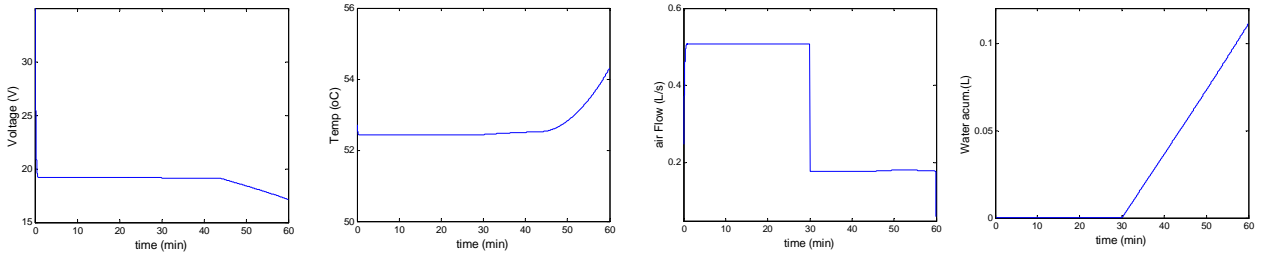


Figure 3. Evolution of variables by fault in the reaction air fan

### 3.2 Fault in the Cooling System

The cooling system maintains temperature within the operating conditions. When temperature increases, the reaction air has a drying effect and reduces the relative humidity (UR). A low UR can have a catastrophic effect on the polymer electrolyte membrane, which not only totally relies upon high water content, but also is very thin (and thus prone to rapid drying out). The drying of the membrane changes the resistance of membrane to proton flow ( $R_M$ ).  $R_M$  is affected by the adjustment of  $\psi$ , which varies according to equation (4):

$$\Psi_{(k)} = \frac{\Psi_{(0)}}{\left(\frac{const_3}{UR_{out(k)}}\right)^2} \quad (4)$$

where,  $const_3$  defines when the membrane is taken to be drying.

The variation of  $R_M$  produces an increase in the  $V_{ohmic}$ , and it produces the reduction of  $V_{FC}$ . Figure 4 illustrates the evolution of the Voltage, Temperature, air Flow, and heat removed by cooling system ( $\dot{Q}_{rem2}$ ), when a total fault in the cooling system is considered at  $t=30$  minutes. The initial fault effect (at  $t=30$  min.) is the increasing of temperature, also affecting the voltage and air flow volume.

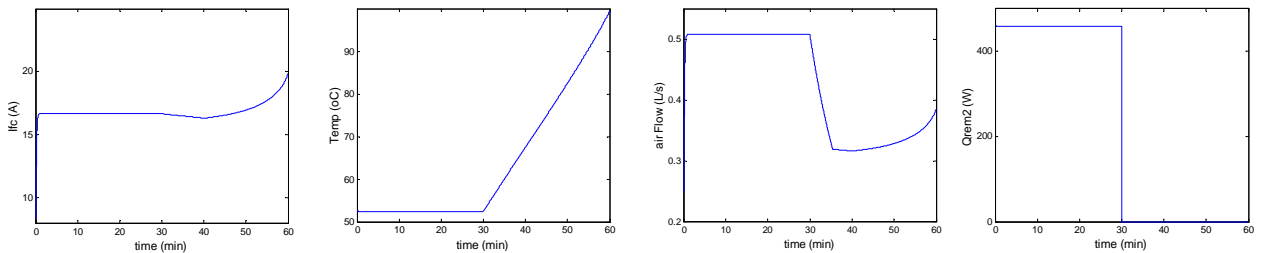


Figure 4. Evolution of variables by fault in the cooling system

### 3.3 Fuel Crossover and Internal Loss Current ( $J_n$ )

There is a small amount of wasted fuel that migrates through the membrane. It is defined as *fuel crossover* -- some hydrogen will diffuse from the anode (through the electrolyte) to the cathode, react directly with the oxygen, and produce no current for the FC.

In normal conditions, the flow of fuel and electrons through the membrane ( $J_n$ ) is very small (aprox.  $0.003\text{A}/\text{cm}^2$ ). A sudden increase in this variable can be associated with either abnormal ion membrane conduction or rupture of membrane.

This variation of  $J_n$  produces an increase in the concentration voltage drop ( $V_{con}$ ), and therefore a reduction of  $V_{FC}$ .

Figure 5 illustrates the evolution of the Voltage, Temperature, air Flow, and  $J_n$  when a sudden variation of  $J_n$  is performed from  $0.003$  to  $0.1$  ( $\text{A}/\text{cm}^2$ ) at  $t=30$  minutes. The effect is a sudden variation on all the variables.

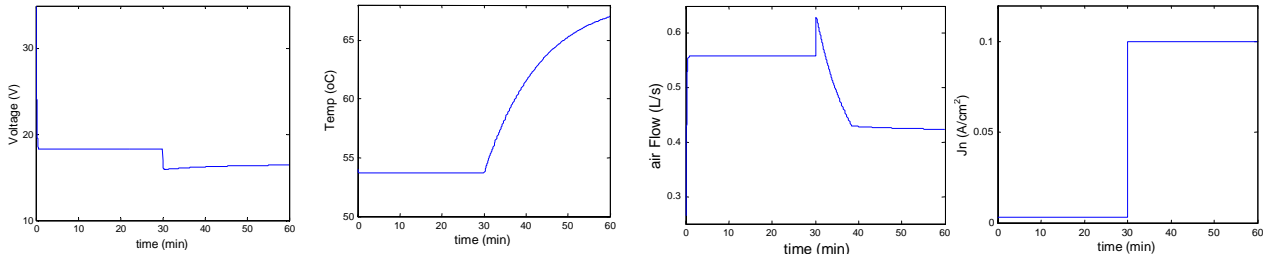


Figure 5. Evolution of variables by variation in  $J_n$ .

### 3.4 Fault in the Hydrogen Feed Line

In general, for mobile and stationary applications, the hydrogen is assumed to be supplied from a high-pressure bottle and reduced by a pressure controller. In normal conditions, the hydrogen pressure is assumed to be constant (1 atm.). The reduction of  $H_2$  pressure decreases the  $E_{Nernst}$ , increases the  $V_{act}$ , and has a corresponding affect on  $V_{FC}$ .

Figure 6 illustrates the evolution of the Voltage, Temperature, air Flow, and  $H_2$  pressure, when a reduction on the  $H_2$  pressure is considered from 1 to 0.2 (atm.) at  $t=30$  minutes. The fault effect is the instant variation on all variables affecting the performance of the FC.

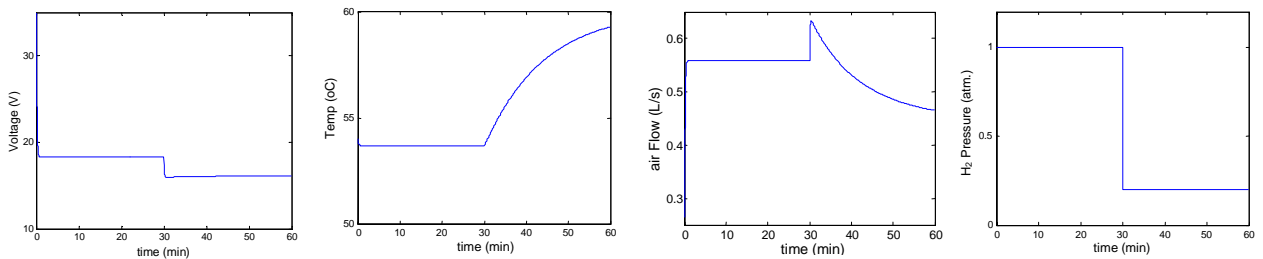


Figure 6. Evolution of variables by reduction in  $H_2$  pressure

In section 3, the effects of four types of faults on the FC operation were explained simply and directly. But, when a fault happens, an interconnected dependence among the variables is performed. That makes diagnosis of the fault cause difficult. Figures 3 through 6 illustrate this dependence, in which at all cases of faults, all the variables have performed changes.

By implementing those types of faults, and their effects, on the mathematical model of the FC, databases for recording the evolution of variables in faulty conditions can be constructed. Then, probabilistic approaches can be applied on the databases to qualify and quantify the dependency relationship among the variables. In the next section, Bayesian networks are considered for the construction of a graphical-probabilistic model based on databases.

## 4. Bayesian Networks for Fault Diagnosis

Bayesian networks have been extensively applied to fault diagnosis, however in the area of fuel cells is a new field. One advantage of Bayesian network is that permits the combination of expert knowledge of the process and probabilistic theory for the construction of a diagnostic procedure; however both are necessary for the construction of a good Bayesian network.

A Bayesian network is a structure that graphically models relationships of probabilistic dependence within a group of variables. A Bayesian network is composed of the network structure and the conditional probabilities. A directed acyclic graph (DAG) represents the structure, where each node of the graph is associated to a variable  $X_i$ , and each node has a set of *parents*  $pa(X_i)$ . The conditional probabilities numerically capture the probabilistic dependence among the variables (Pearl, 1989).

The construction of a graph to describe a diagnostic process can be executed in two ways:

- Based on human knowledge about the process, where relationships among variables are established to define the criteria for choosing the next state (i.e. the relationship between variables and parents);
- Based on probabilistic methods using databases of records.

The construction of a Bayesian network based on knowledge can be relatively simple; but its efficacy depends completely on the human expert knowledge about that domain.

The implementation of probabilistic methods for the structure learning can follow two approaches: constraint-based and search-and-score. In the constraint-based approach, the starting point is an initially given graph. And then, edges are removed or added if certain conditional independencies are measured in the database. In the search-and-score approach, a search through the space of possible DAGs is performed for finding the best DAG. In this research, the Bayesian-Score (K2) (Cooper et. al. 1992) and Markov Chain Monte Carlo (MCMC) (Pearl, 2000) algorithms are applied.

In this work, the construction of a Bayesian network for fault diagnosis begins with the generation of a graph applying probabilistic methods, and after that refined using the domain knowledge. The complete sequence consists of the following steps:

- Construction of the database -- the records are provided from a mathematical model of a PEMFC implemented on MatLab<sup>®</sup>. Field experiments could also provide those records, however two major problems should be considered, i) big amount of data are necessary, and ii) variables such as  $Q_{gen}$ , Flooding, and  $\lambda$ , impose additional challenges to be monitored.
- Implementation of search-and-score algorithms (K2 and MCMC) to find the initial structure -- the probabilistic approaches were implemented using the BNT (Bayesian Network Toolbox) developed for Matlab (Murphy, 2002).
- Constraint-based conditions are applied for improving the structure where knowledge about the conditions of independence among variables is applied.
- Calculation of conditional probabilities -- the conditional probabilities are calculated on the resulting structure.

#### 4.1 Generation of the Database

Binary states of the variables are considered (0=normal, 1=abnormal). The general procedure is to monitor a specific variable. If after a fault, the value of such variable is off a certain tolerance band, then a flag should be turned to "1".

The next step is the construction of a vector containing the value of all variables. This vector corresponds to a single case in the database with values of all variables. From the mathematical model, the evolution of some variables that can be difficult to monitor on a real machine (such as  $Q_{gen}$  or  $UR$ ) can be observed. Records of all variables are essential for the construction of the network structure avoiding hidden variables. A database with 10,000 cases was constructed for the structure learning of a Bayesian network for fault diagnosis in this fuel cell system.

#### 4.2 The Bayesian-Score (K2) Algorithm

Initially in the K2 algorithm, each node has no parents. It then incrementally adds those parents whose addition most increases the score of the resulting structure. When the addition of no single parent increases the score, it stops adding parents to the node. Before the algorithm begins, the parents of every variable must be defined. Therefore, the human-expert experience is important to define that order.

Figure 7-a) illustrates the resulting network structure applying the K2 algorithm. The order of the variables is the following:  $J_n=1$ ,  $aF=2$ ,  $rF=3$ ,  $H_2=4$ ,  $Flow=5$ ,  $Q_{gen}=6$ ,  $\lambda=7$ ,  $Flooding=8$ ,  $Drying=9$ ,  $UR_{out}=10$ ,  $Overload=11$ ,  $Voltage=12$ ,  $I_{FC}=13$ ,  $Temperature=14$ ,  $Power=15$  (difference between real output power and required load),  $pH_2=16$ . For example, according to Figure 7-a), a probabilistic dependence among variable 1 (as parent) and variables {2, 3, 4, 6, 9, 10 and 11} (as children) is established from the database.

#### 4.3 The MCMC (Markov Chain Monte Carlo) Algorithm

The MCMC algorithm starts at a specific point in the space of DAGs. The search is performed through all the nearest neighbors, and it moves to the neighbor that has the highest score. If no neighbor has a higher score than the current point, a local maximum was reached, and the algorithm stops. A neighbor is the graph that can be generated from the current graph by adding, deleting or reversing a single arc. Figure 7-b) illustrates the resulting network structure applying the MCMC algorithm where the variable order is the same as in Figure 7-a).

#### 4.4 Improving the Network Structure

In practice, the search-and-score algorithms are not exact, and used only as initial approximations. Also since the K2 and MCMC algorithms applied different tradeoffs for searching the structure, those algorithms can produce different results. To improve the network structure, the following steps are executed:

- Fusion of the results applying the K2 and MCMC algorithms
- Groups of variables are arranged in layers
- Application of constrains on the structure based on domain knowledge

The fusion of the results applying K2 and MCMC basically confirms the edges present in both structures and submits the remained edges to be erased based on constrains and domain knowledge.

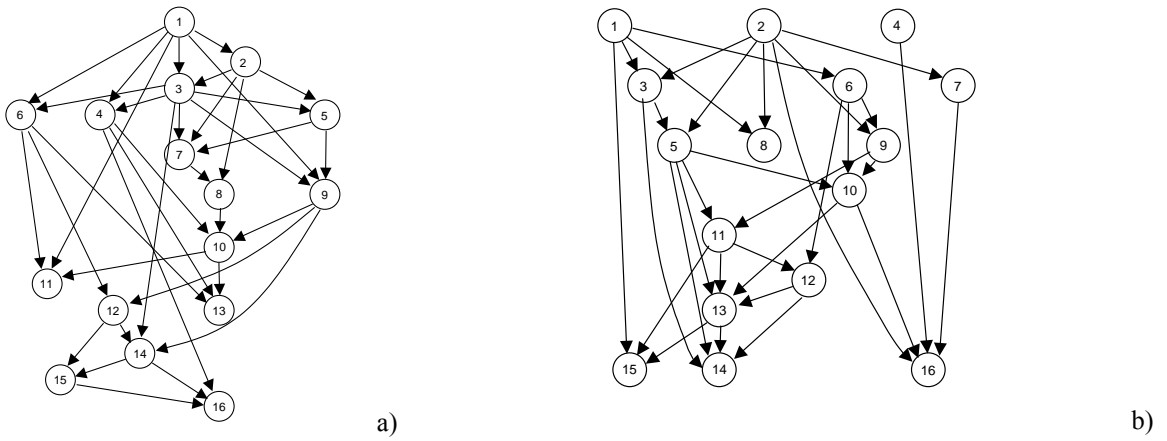


Figure 7. Bayesian network structure, a) Applying the K2 algorithm, b) Applying the MCMC algorithm.

In this structure, three layers are considered: fault causes, pattern recognition, and sensors. Fault causes are the possible causes of faults such as faults in the air reaction fan and cooling system, growth of  $J_n$ , and low  $H_2$  pressure. Sensors are variables that can be easily monitored using sensors (such as voltage, electrical current, temperature, power, and  $H_2$  pressure). Pattern recognition is associated with variables difficult to monitor in a real machine, but that play an important role in a cause-effect structure and define a pattern of fault.

Some of the constraints to consider are: i) independence among the fault causes ( $J_n$ ,  $aF$ ,  $rF$ ,  $H_2$ ), where only one fault takes place each time and one fault cause does not influence other fault causes; ii) independence among sensors ( $Power$ ,  $I_{FC}$ ,  $Volt$ ,  $T$ ,  $pH_2$ ) where the monitored variable is not influenced by other variable states, only by the effects monitored by itself. Figure 8 illustrates the resulting Bayesian structure.

The probabilities in Bayesian networks define the probability distribution of a node given its parents. In this research the maximum posteriori likelihood algorithm (Pearl, 1989) was applied.

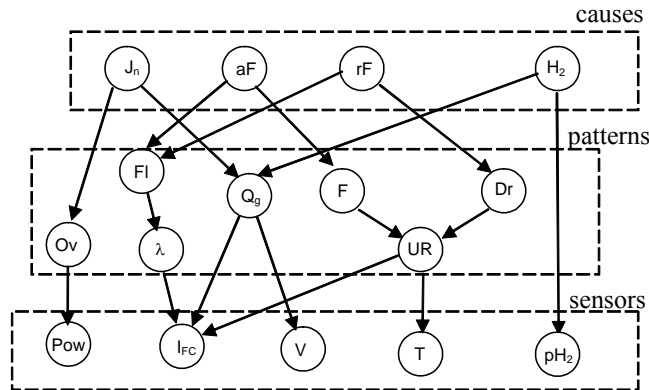
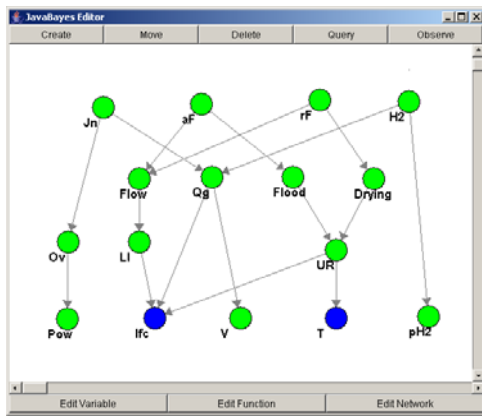


Figure 8. Network structure for fault diagnosis in a PEMFC

#### 4.5 Inference Calculation

There are many different algorithms for calculating the inference in Bayesian networks, which apply different tradeoffs between speed, complexity, generality, and accuracy (Pearl, 1989). The variable elimination algorithm permits the inference calculation on a Bayesian network with a generic structure. The JavaBayes System (Cozman, 2001) implements this algorithm on a graphic interface. Figure 9 illustrate the utilization of this program for the inference calculation for fault diagnosis in FCs. Figure 9-a) depicts the graphical representation of the Bayesian structure. In this case, electrical current ( $I_{FC}$ ) and temperature ( $T$ ) are the evidence observed, (i.e.  $I_{FC}=1$  and  $T=1$  indicate a type of abnormal situation). In Figure 9-b), the conditional probabilities have been calculated for all fault causes ( $J_n$ ,  $aF$ ,  $rF$ , and  $H_2$ ). In this case, when  $I_{FC}=1$  and  $T=1$  the most probable fault cause is  $aF$  (reduction in air reaction Flow) with 94% probability. The causes  $rF$  and  $J_n$  have intermediary probabilities, 39% and 34%, respectively. And cause  $H_2$  has the least probability: 4%.

Network structures representing a diagnostic process play a fundamental role for fault tolerant machines since they can be associated with fault treatment processes, (i.e. performing the fault diagnosis to identify the fault cause and executing the automatic recovery process). Riascos, et al. (2004) have analyzed the fault detection and fault treatment by automatic recovery processes in electric autonomous guided vehicles (AGV) and machining processes.



a)

```

JavaBayes Console
File Options Help
Posterior distribution:
probability ( "Jn" ) { #1 variable(s) and 2 values
table
0.3459876746073625 // p(true | evidence )
0.6540123253926375; // p(false | evidence );
}
Posterior distribution:
probability ( "aF" ) { #1 variable(s) and 2 values
table
0.7475274420645679 // p(true | evidence )
0.2524725579354322; // p(false | evidence );
}
Posterior distribution:
probability ( "rF" ) { #1 variable(s) and 2 values
table
0.38998659582768963 // p(true | evidence )
0.6100134041723103; // p(false | evidence );
}
Posterior distribution:
probability ( "H2" ) { #1 variable(s) and 2 values
table
0.04563026894053219 // p(true | evidence )
0.9543697310594678; // p(false | evidence );
}

```

b)

Figure 9. The JavaBayes System, a) Bayesian structure, b) Inference calculation

## 5. Conclusion

The construction of a network structure for fault diagnosis in proton exchange membrane fuel cells (PEMFC) was executed implementing probabilistic approaches.

Fault records of some variables were constructed including variables difficult to monitor on a real machine. The record of all relevant variables is essential for the construction of the network structure avoiding hidden variables, especially on intermediary layers.

For the construction of a network structure, the sole implementation of probabilistic approaches, (such as the K2 and MCMC algorithms), is not enough for the construction of a “good” network, as presented in Figure 7. An understanding of the process, (e.g. processes in an PEMFC), is necessary, particularly for applying constrain-based conditions based on knowledge to improve the network structure.

For the diagnostic process, (i.e. the inference calculation), the evidence was based on observations of variables that can be easily monitored by sensors like voltmeters, ammeters, thermocouples, etc. This permits an easy implementation of fault diagnostic processes in an FC system.

The tests have shown agreement between the inference results and the original fault causes. They will permit implementation of an on-line supervisor for fault diagnosis applying Bayesian networks constructed as described in this research.

Topics such as the study of fault effects in FCs, the construction of network structures for fault diagnosis in FCs, and their association to fault treatment processes are still under study, and are still open to research contributions.

## 6. Acknowledgment

The authors thank CNPq and FAPESP for financial support.

## 7. References

- Cooper, G.F., Herskovits, E., “A Bayesian method for the induction of probabilistic networks from data,” *Machine Learning*, n.9, pp.309-347, 1992.
- Cozman, F.G., 2001, <http://www-2.cs.cmu.edu/~javabayes/>
- Corrêa, J.M., Farret, F.A., Canha, L.N., Simões, M.G., “An electrochemical-based fuel cell model suitable for electrical engineering automation approach,” *IEEE Transactions on Industrial Electronics* – accepted for publication.
- Corrêa, J.M., Farret, F.A., Gomes, J.R., Simões, M.G., “Simulation of fuel cell stacks using a computer-controlled power rectifier with the purpose of actual high Power injection applications,” *IEEE Transactions on Industrial Applications Society*, July/August, vol.39, n. 4, pp. 1136-1142, 2003.
- Corrêa, J.M., Farret, F.A., Canha, L.N., Simões, M.G., Popov, V.A., “Sensitivity analysis of the modeling parameters used in simulation of proton exchange membrane fuel cells,” *IEEE Transactions on Energy Conversion* – accepted for publication.
- Larminie, J., Dicks, A., “*Fuel Cell Systems Explained*”, John Wiley & Sons Ltd. 2000.
- Murphy, K., 2002, <http://www.ai.mit.edu/%7Emurphyk/Software/BNT/bnt.html>
- Pearl, J., “*Causality: Models Reasoning and Inference*”, Cambridge University Press. 2000
- Pearl, J., “*Probabilistic Reasoning in Intelligent Systems: Networks of Plausible Inference*”, Morgan Kaufmann Publ. 1989.
- Riascos, L.A.M., Moscato, L., Miyagi, P.E., “Detection and treatment of faults in manufacturing systems based on Petri nets,” in: *RBCM (Revista Brasileira das Ciências Mecânicas)*, v. XXVI, n.3, July-September 2004.